Low-spin structure of the N=82 nucleus ^{137}Cs

W. Reviol, D. G. Sarantites, J. M. Elson, J. E. Kinnison, A. Gargano, R. V. F. Janssens, J. M. Allmond, A. D. Ayangeakaa, S. Bottoni, M. P. Carpenter, H. M. David, A. Galindo-Uribarri, N. Itaco, T. Lauritsen, E. Padilla-Rodal, and S. Zhu

Phys. Rev. C **98**, 014328 — Published 30 July 2018

DOI: 10.1103/PhysRevC.98.014328

Low-spin structure of the $N = 82$ nucleus ^{137}Cs

W. Reviol[1], D. G. Sarantites[1], J. M. Elson[1], J. E. Kinnison[1],
A. Gargano[2], R. V. F. Janssens[3,4], J. M. Allmond[5], A. D. Ayangeakaa[6],*
S. Bottoni[6,7], M. P. Carpenter[6], H. M. David[6],† A. Galindo-Uribarri[5],
N. Itaco[2,8], T. Lauritsen[6], E. Padilla-Rodal[9], and S. Zhu[6]

[1]*Department of Chemistry, Washington University, St. Louis, MO 63130, USA*

[2]*Istituto Nazionale di Fisica Nucleare,*
Complesso Universitario di Monte S. Angelo, Via Cintia, I-80126 Napoli, Italy

[3]*Department of Physics and Astronomy,*
University of North Carolina at Chapel Hill, Chapel Hill, NC 27599, USA

[4]*Triangle Universities Nuclear Laboratory, Durham, NC 27708, USA*

[5]*Physics Division, Oak Ridge National Laboratory, Oak Ridge, TN 37831, USA*

[6]*Physics Division, Argonne National Laboratory, Argonne, IL 60439, USA*

[7]*Universita degli Studi di Milano, Via Celoria 16, Milano 20133, Italy*

[8]*Dipartimento di Matematica e Fisica,*
Universitá degli Studi della Campania "Luigi Vanvitelli"
viale Abramo Lincoln 5, I-81100 Caserta, Italy

[9]*Instituto de Ciencias Nucleares, UNAM, 04510 Mexico City, Mexico*

(Dated: May 29, 2018)

Abstract

Excited states in ^{137}Cs have been studied by using the near-barrier, single-proton transfer reaction ^{10}B(^{136}Xe,^{9}Beγ)^{137}Cs in inverse kinematics and performing particle-γ and particle-$\gamma\gamma$ coincidence measurements. The low-spin level scheme of ^{137}Cs has been augmented: *(i)* The expected set of single-proton, seniority $\upsilon = 1$ states has been delineated in its entirety; *(ii)* Another member of the $\upsilon = 3$ proton $0g_{7/2}$ multiplet, a low-lying $9/2^+$ level, has been identified and this set of states now approaches completion; *(iii)* A second $9/2^+$ and a candidate $13/2^+$ level have been observed. The results are discussed in the framework of shell-model calculations in the proton $2s1d0g0h$ shell.

PACS numbers: 27.80.+w, 27.90.+b, 23.20.Lv, 21.60.Ev

*Present address: Department of Physics, U.S. Naval Academy, Annapolis, MD 21402, USA

†Present address: Gesellschaft für Schwerionenforschung, Darmstadt, Germany

I. INTRODUCTION

Studies of increasingly neutron-rich nuclei lead to the quest for new and improved data on single-proton states [1]. Specifically, it is desirable to use a complete set of experimentally supported single-particle proton energies, for a given valence-proton shell, when describing high-precision spectroscopic data. In the ^{132}Sn region, for example, the nuclei of interest are those from Sb ($Z = 51$) up to about Cs ($Z = 55$) with neutron numbers $N \geq 82$.

The subject of the present study is the semimagic nucleus ^{137}Cs. Recent experimental studies of ^{137}Cs have been carried out with emphasis on the high-spin yrast structure, using deep-inelastic, one-proton transfer, and fusion-fission reactions [2, 3] as well as spontaneous fission of ^{252}Cf [4]. The most comprehensive low-spin studies, on the other hand, date back to the nineteen-seventies using (d,^{3}He) and (^{3}He,d) reactions [5] as well as β decay [6, 7]. The resulting level scheme is proposed in Ref. [8]. The present experiment utilizes a one-proton transfer reaction in inverse kinematics with a ^{136}Xe beam on a ^{10}B target. Using the approach of Refs. [9, 10], a specific target-like fragment (TLF) is correlated with coincident γ rays emitted by the corresponding projectile-like fragment (PLF). New levels in ^{137}Cs as well as spin and parity assignments to previously observed states are reported. The experimental findings are compared with shell-model calculations. The overall agreement between theory and experiment is found to be satisfactory.

II. EXPERIMENTAL CONDITIONS AND ANALYSIS PROCEDURES

The experiment introduced above was performed at the ATLAS accelerator at Argonne National Laboratory as part of a series of runs with a 560-MeV ^{136}Xe beam impinging on different targets. The pertinent information about these runs is summarized in Table I. The detection setup comprised Digital Gammasphere [11], with 92 Compton-shielded HPGe detectors arranged in 16 angular rings around the target [12], and the Phoswich Wall charged-particle detector array [13], located downstream from the target with a laboratory-angle coverage of $9^\circ \leq \theta_{lab} \leq 72^\circ$. The event trigger required that a Phoswich Wall element and at least two HPGe detectors fired prior to suppressing Compton-scattering signals.

In the offline analysis, a gating procedure was applied to the so-called (A,C) particle map, which makes use of the Phoswich Wall fast-plastic and CsI(Tl) signals [13], and the prompt

peak of the measured particle's time spectrum with respect to the accelerator radiofrequency. The map gating condition required the presence of TLF beryllium events. A typical particle map for the data obtained with the ^{10}B target is presented in Fig. 1. The Doppler-shift correction applied to the γ-ray spectra relied on the PLF velocity vector reconstructed event-by-event for the direct reaction, and took advantage of the 256-fold pixelation of the Phoswich Wall [13].

For each run, two types of two-dimensional histograms of γ-ray energies were created: *(i)* a $E_\gamma - E_\gamma$ matrix and *(ii)* a set of "angle-dependent" $E_\gamma(\chi) - E_\gamma(\text{any})$ matrices. The matrices in *(ii)* allowed to determine the γ-ray anisotropies relative to the spin direction of the fragment nucleus following the procedure of Ref. [14]. Here, χ represents the angle between the emitted γ ray and the spin direction (binned into 10° increments), while "any" stands for no angle requirement. All these histograms were analyzed using the RADWARE analysis package [15].

III. EXPERIMENTAL RESULTS

This section reports the new information on the ^{137}Cs level scheme obtained in the present experiment. Representative γ-ray spectra for the desired one-proton transfer channel leading to ^{137}Cs are provided in Figs. 2 and 3, and are used to justify the location of new transitions in the level scheme of Fig. 4. Note that the precise level and γ-ray energies are reported in Table II, together with other relevant information on each transition. The total projection in panel (a) of Fig. 2 has been produced with a beryllium gate and is dominated by the γ rays of ^{137}Cs such as the prominent $5/2^+ \rightarrow 7/2^+$ ground-state transition [8]. In addition to ^{137}Cs, the ^{139,140}Ba, ^{139}La, and ^{142}Ce nuclei are present as well. The latter nuclei originate from incomplete fusion reactions, for which the remaining light fragments have leaked into the particle coincidence gate. Specifically, the ^{136}Xe + α incomplete fusion reaction leads to the ^{139}Ba + n and ^{140}Ba channels, and a ^{6}Li ion remains, while the ^{136}Xe + ^{6}Li combination produces ^{139}La + 3n and is accompanied by an α particle. In this context, the ^{142}Ce line is attributed to a ^{136}Xe reaction on oxygen, with the latter being present due to target oxidation.

Panels (b) and (c) display beryllium- and γ-gated spectra for ^{137}Cs. The spectrum in coincidence with the 455-keV transition [panel (b) and inset of panel (c)] displays the expected

lines [8] and, in addition, new γ rays with respective energies of 666, 1037, 1703, and 1905 keV. Except for the 666-keV γ ray, these transitions directly feed the 455-keV first-excited state in ^{137}Cs, as proposed in Fig. 4. The 666-keV γ ray represents the energy difference between the 1703- and 1037-keV transitions. These three lines determine the position of the second $1/2^+$ state more precisely than was the case in previous work (17-keV uncertainty [5, 8]). Further justification of the above direct feeding of the first excited state is provided by the 1273-keV gate of panel (c): this ground-state transition and the 455-keV γ ray do not share coincidence relationships with other lines. The spectrum of Fig. 2 (b) warrants two additional comments. Firstly, the present data support the negative result of Ref. [7] on a low-lying candidate $3/2^+$ level at 982 keV that had been reported in a preceding study [6]. If this level had been populated, it would likely decay to the 455-keV state, but a corresponding $E_\gamma \sim 527$-keV transition is absent. Secondly, the presence of additional transitions feeding the 455-keV state with respective energies of 1119, 1328 or 1461 keV [6, 7] is not confirmed by the present data. Such a 1119-keV γ ray would form a triplet with the 1109- and 1114-keV transitions, however, this peak does not have the unusually broad width that would suggest the presence of three close-lying transitions of comparable strength. Similarly, Fig. 2 (b) is lacking evidence for possible 1328- and 1461-keV lines.

Figure 3 (a) provides the coincidence spectrum gated by the 1114-keV transition. This spectrum highlights the sequence of the prominent 455-, 1114-, and 298-keV transitions. It is consistent with both the aforementioned absence of a 1119-keV line (hence, absence of a higher-lying γ ray other than that with $E_\gamma = 298$ keV), and the placement of the 1037-, 1109-, 1197-, 1703-, and 1905-keV lines with respect to their common final state. The inset of Fig. 3 (a) displays the coincidence spectrum gated by the 1109-keV transition, and serves as a comparison, with the 298-keV line being notably absent. Panel (b) provides the coincidence spectrum gated by the 1184-keV ground-state transition, herewith focusing on the yrast sequence of the ^{137}Cs level scheme ($I^\pi > 11/2^+$). Strong evidence is found for the 487- and 222-keV transitions from the confirmed $15/2^+$ and $17/2^+$ levels (see below) and for a new 627-keV line. Additional γ rays are those with $E_\gamma = 373$, 861, and 684 keV. The latter is weak, but its placement as a "feeder" of the 1184-keV level appears to be justified. A spectrum gated by the 627-keV transition is presented in panel (c): of the yrast transitions it displays only the 1184-keV line, suggesting the presence of a 1811-keV level from which the new γ ray decays. The weak 455-keV peak present in this spectrum can be due to a

somewhat poorer background subtraction (hence, a small fraction of the strongest γ ray remains) or to a transition in ^{139}Ba. The former possibility is more likely, since the 455-keV gate of Fig. 2 (b) does not indicate any ^{139}Ba line. In addition, there is no $E_\gamma \sim 730$-keV transition that would link the 1184- and 455-keV levels.

For almost all the observed levels, spin and parity assignments are proposed based on a γ-ray angular-distribution analysis. Figure 5 provides sample angular distributions for three γ rays: a known stretched electric quadrupole ($E2$) (a) and antistretched magnetic dipole ($M1$) transition (b), and the 1273-keV line, subject of a new assignment (c). These have been fitted with a standard Legendre polynomial expression and the fit results are included in the figure. The characteristic A_2/A_0 and A_4/A_0 coefficients derived from the fits are reported in the last two columns of Table II. The values obtained for the known transitions [Fig. 5 (a) and (b)] are in line with expectations for the present analysis, using the spin-alignment method, where stretched (or antistretched) dipole and quadrupole transitions have positive and negative A_2/A_0 coefficients, respectively. The positive-parity assignment for the state associated with the 455-keV transition (hence, of $M1$ character) is adopted from Ref. [5]: this level has been shown to contain most of the $d_{5/2}$ single-particle strength.

The 849- and 1273-keV antistretched/stretched dipole transitions to the ground state have not only positive A_2/A_0 coefficients, but also non-zero A_4/A_0 ones indicative of a mixed multipole character of the $M1 + E2$ type. The 849-keV transition is bypassed by the 393-keV γ ray, the latter having a negative A_2/A_0 coefficient. For the common $E =$ 849-keV initial state, a $5/2_2^+$ assignment follows since the angular distribution of the 393-keV γ ray is consistent with that of an unstretched-dipole transition (no spin change). For the 1273-keV transition, a stretched-dipole assignment is preferred over an antistretched one; otherwise one must invoke the rather unlikely scenario of the presence a third low-lying $5/2^+$ state. Hence, a $9/2^+$ assignment is proposed for the 1273-keV level. For the 1612-keV transition, which decays to the first excited state, different considerations apply, and its angular distribution is provided in Fig. 6 (a). This transition has A_2/A_0 and A_4/A_0 coefficients suggesting a $3/2^+$ assignment for the initial state at 2067 keV. Specifically, the A_4/A_0 coefficient is consistent with 0 and, thus, favors the $3/2^+$ assignment over the $7/2^+$ alternative [16]. This new assignment removes the previous $(3/2^+, 5/2^+)$ ambiguity for the $E = 2067$-keV level [8], in particular a $5/2^+$ assignment is ruled out.

Among the other prominent transitions feeding the $E = 455$-keV, $5/2^+$ state are the 1037-

and 1703-keV γ rays, which are both isotropic as indicated by A_2/A_0 coefficients consistent with 0. This observation supports the assignment for the $E = 1492$- and 2158-keV levels as the first and second $1/2^+$ state, respectively [8]. The 666-keV γ ray connecting these levels is too weak to enable an additional angular-distribution measurement. Nevertheless, the observation of this γ ray in the presence of the bypassing 1703-keV $E2$ transition is in line with the $1/2^+_{1,2}$ assignments; these states have apparently similar wavefunctions. The 1197-keV γ ray feeding the $E = 455$-keV, $5/2^+$ state has a negative A_2/A_0 coefficient and, thus, can be either of stretched-quadrupole or unstretched-dipole character. The corresponding level at 1652 keV is tentatively assigned $(5/2, 9/2)$, indicating that its spin cannot be unambiguously determined. For the 1109- and the weak 1905-keV γ rays, no angular distribution is available.

The spin-parity assignments for the 1570- and 1868-keV levels share certain considerations and, thus, are discussed together. The angular distributions of some of the γ rays involved in the deexcitation of the two states, those with $E_\gamma = 1114$ and 298 keV, are presented in Fig. 6 (b) and (c), respectively. The 1114-keV γ ray and its bypassing 1570-keV transition to the ground state have sets of A_2/A_0 and A_4/A_0 coefficients suggesting a $9/2^+_2$ or a $5/2^+_3$ assignment for the $E = 1570$-keV initial state. Both the 298- and 594-keV γ rays are characterized by a A_2/A_0 coefficient compatible with a stretched-dipole assignment and, furthermore, by a A_4/A_0 coefficient consistent with 0. This common feature suggests that the 298- and 594-keV dipole transitions are rather pure and, thus, of the $E1$ type (negligible $M2$ components). In addition to the angular-distribution analysis, the following considerations apply: *(i)* Only the $9/2^+_2$ and $11/2^-$ assignments for the respective 1570- and 1868-keV levels appear to be consistent with the γ-ray coincidence relationships; a scenario invoking instead a $5/2^+_3$ and, accordingly, a $7/2^-$ level would imply that a $E_\gamma \sim 1413$-keV transition between the $E = 1868$- and 455-keV levels should be present, and this possibility is excluded as can be seen in the spectrum of Fig. 2 (b); *(ii)* The scenario with a $E = 1868$-keV, $7/2^-$ level also leads to a $E_\gamma \sim 1868$-keV ground state transition; although such a γ ray (without a coincidence relationship with any other line) is hard to identify, there is no hint for a $\sim$ 1868-keV photon, and this weakens the possible alternative further. On the other hand, the lack of evidence for a ~ 1868-keV γ ray also supports the $11/2^-$ assignment for the 1868-keV level: the corresponding ground-state transition would be of $M2$ character and would be a rather unlikely competitor of the other decay branches. It should be pointed out that

there is some ambiguity in the literature regarding the spin-parity quantum numbers for the 1868-keV state. This level was originally characterized as a $\ell = 5$ (i.e., $h_{11/2}$) state in Ref. [5]. This result was subsequently adopted in Refs. [6, 7], but the compilation of Ref. [8] assigned spin-parity $9/2^-$ without providing a basis for the assignment. The new evidence presented here requires $11/2^-$ quantum numbers for the 1868-keV level, in line with Ref. [5].

In the present study, the assignments of some of the yrast transitions [3] have been confirmed as well. The A_2/A_0 coefficients of the 1184- and 487-keV lines indicate that both transitions are of $E2$ character, whereas the set of A_2/A_0 and A_4/A_0 values obtained for the 222-keV γ ray suggests that the next higher yrast transition is of the $M1+E2$ type (although the A_4/A_0 coefficient is not much different from 0). The 1811-keV level is assigned a 13/2 spin, primarily based on the positive A_2/A_0 coefficient obtained for the angular distribution of the 627-keV transition (Table II). An alternative 9/2 assignment is excluded, as it would imply the possibility of a bypassing $E_\gamma \sim$ 1811-keV ground-state transition, which can be ruled out. Due to the large error of the A_4/A_0 coefficient for the new transition, no parity assignment is proposed. Nevertheless, the near-yrast 1811-keV level can be viewed as a candidate for the $13/2^+$ state (see Sec. IV).

It is worthwhile to mention that the $E = 1893$-keV, $17/2^+$ level is the highest-spin state observed with the present reaction. For example, the rather prominent 890-keV, $21/2^+ \rightarrow 17/2^+$ yrast transition of Refs. [2–4] is absent [cf. Fig. 3 (b)]. Evidently, the single-proton transfer reaction favors the population of sets of low-spin, non-yrast states in ^{137}Cs, which are, thus, complementary to those studied in Refs. [2–4].

IV. DISCUSSION

In this section, a comparison is made between the low-spin ($I \leq 17/2$) levels of ^{137}Cs and the results of shell-model calculations for this nucleus. In addition, level systematics for ^{137}Cs and neighboring $N = 82$ nuclei are presented as a function of proton number.

Table III compares the calculated level energies with those obtained from the present experiment. In these calculations, a ^{132}Sn closed core was chosen and the valence-proton space included the single-particle orbitals of the $50 - 82$ shell; i.e., $0g_{7/2}, 1d_{5/2}, 1d_{3/2}, 2s_{1/2}$, and $0h_{11/2}$. The calculations employed the two-body effective Hamiltonian of Ref. [17]

with the matrix elements derived from the CD-Bonn nucleon-nucleon potential [18], and the single-particle energies taken from the experimental spectrum of ^{133}Sb, except for the $2s_{1/2}$ orbital, which was not identified in this nucleus. The $2s_{1/2}$ energy was based on the more precisely determined $1/2_2^+$ level of ^{137}Cs reported in Table II.

In addition to the calculated level energies, the table specifies, in the third column, the dominant configuration of the state, which typically represents $\geq 65\%$ of the total amplitude of the wavefunction (the higher-lying $3/2^+$ states are the exception). The configuration is expressed as a coupling between, on the one hand, the ground state or one of the lowest-lying excited states of the even-mass ^{136}Xe isotone and, on the other, the single-particle state of the remaining valence proton. Here, the couplings involving the 0_1^+ state of ^{136}Xe represent the single-proton states, all the other cases are associated with 3 "unpaired" protons (see discussion below).

Overall, there is a satisfactory correspondence between calculated and observed levels, with discrepancies of 150 keV or less, except for the $1/2_1^+$ and $3/2_2^+$ states. The largest discrepancy (293 keV) occurs for the $3/2_2^+$ level, where the calculated energy is also lower than the observed one. This appears to be the result of dealing with a strongly mixed configuration (cf. footnote c of Table III). The overall picture validates the choice of ^{132}Sn as the inert core. Two additional comments on specific states can be made.

(i) The 3/2$^+$ states and a related issue: The calculated $3/2_1^+$ level remains unobserved, and the $3/2_2^+$ state is calculated to be of mixed $0_1^+ \otimes 1d_{3/2}$ and $2_1^+ \otimes 1d_{5/2}$ character. On the other hand, the $B(M1)$ values calculated in the course of the present study predict the $3/2_2^+ \rightarrow 5/2_1^+$ transition to be comparatively strong (see footnote b of Table III), as the initial- and final-state wavefunctions have significant $0_1^+ \otimes 1d_{3/2}$ and $0_1^+ \otimes 1d_{5/2}$ components, respectively. Unfortunately, the present data do not provide valuable lifetime information. Nevertheless, the corresponding 1612-keV γ ray is one of the strongest $M1$ transitions in the spectra, and this observation appears to be consistent with the above prediction. Also, a possible $9/2_2^+ \rightarrow 7/2_2^+$ transition has a calculated large $B(M1)$ value (footnote a of Table III). While a $7/2_2^+$ state could not be firmly established, the 1564-keV level of Fig. 4 is a possible candidate for this excitation. In this scenario, the transition under consideration would not be observed due to its low energy, in agreement with the present data.

(ii) The 13/2$^+$ state: The observed 1811-keV level is a good candidate for association with the computed $13/2^+$ state due to the proposed spin assignment and an energy difference

between the data and calculations of 142 keV. One of the nearby $N = 82$ isotones, ^{141}Pr, also has a low-lying ($E = 1767$ keV) $13/2^+$ level [19], and it is interesting to compare the decay branches from the $13/2^+$ states in both nuclei. The ^{141}Pr nucleus has a low-lying ($E = 1118$ keV) $11/2^-$ state to which the $13/2^+$ level decays most strongly, but the $13/2^+ \rightarrow 11/2^+$ transition is the next strongest decay branch. Such a $11/2^-$ level is not an option for a deexcitation in ^{137}Cs ($E = 1868$ keV), and the $13/2 \rightarrow 11/2^+$, 627-keV decay path thus mirrors the ^{141}Pr observation, herewith increasing the confidence in the proposed spin assignment for the 1811-keV level.

As is customary for a semi-magic nucleus, most of the ^{137}Cs low-spin levels can be grouped according their seniority [21]. These are, in principle, the *(i)* single-proton, seniority $\upsilon = 1$ states, and $\upsilon = 3$ excitations with a $0g_{7/2}$ broken pair coupled to a proton in the *(ii)* $0g_{7/2}$ or *(iii)* $1d_{5/2}$ orbital; the latter are called $\upsilon = 3$ $0g_{7/2}$ and $\upsilon = 3$ $0g_{7/2}1d_{5/2}$ multiplets, respectively. In order to confirm that the seniority scheme is appropriate, a separate set of shell-model calculations for ^{137}Cs was performed, from which the expected seniority composition of the wavefunctions under discussion was validated. These findings can be summarized as follows: *(i)* States that are characterized by a large ($> 90\%$) $\upsilon = 1$ component are the $7/2^+$ ground state and the $1/2^+_2$, $5/2^+_1$, and $11/2^-$ levels of Table III. As far as the $3/2^+_2$ state is concerned, it turns out that this is a mixture of the $\upsilon = 1$ component and the $\upsilon = 3$ $0g_{7/2}1d_{5/2}$ multiplet. *(ii)* The $\upsilon = 3$ $0g_{7/2}$ multiplet contains the $3/2^+_1$, $5/2^+_2$, $9/2^+_1$, $11/2^+_1$, and $15/2^+_1$ states where the corresponding compositions are typically $\sim 90\%$ (e.g., for $3/2^+_1$, $5/2^+_2$). *(iii)* The $\upsilon = 3$ $0g_{7/2}1d_{5/2}$ multiplet involves the $1/2^+_1$, $5/2^+_3$, $7/2^+_2$, $9/2^+_2$, $11/2^+_2$, $13/2^+$, $15/2^+_2$, and $15/2^+_1$ levels with typical compositions of $\sim 80\%$ (e.g., for $1/2^+_1$).

This seniority description is illustrated in Fig. 7, where a compilation of the lowest-spin levels in ^{137}Cs and in the lighter $N = 82$ isotones can be found. Note that, for ^{137}Cs, only states with firmly established spin and parity have been compiled, whereas for ^{135}I and ^{133}Sb, any state with a proposed spin value is considered. The $\upsilon = 1$ states in ^{137}Cs have all been observed and their decay modes characterized. Similarly, the observation of the $\upsilon = 3$ $0g_{7/2}$ multiplet in ^{137}Cs approaches completion; i.e., only the $3/2^+$ member remains unobserved. With respect to the remaining ^{137}Cs levels, an additional comment is warranted. The $1/2^+_1$ and $7/2^+_2$ states are part of the $\upsilon = 3$ $0g_{7/2}1d_{5/2}$ multiplet, and the $13/2$ and $17/2^+$ levels (cf. Fig. 5) that are also associated with this group (Fig. 7) have been omitted in the last figure only to simplify the presentation. The sets of levels for ^{135}I and ^{133}Sb (Fig. 7) illustrate

the sparsity of experimental information as one moves towards nuclei with a larger neutron excess. Hence, this compilation establishes only the trend of the $5/2_1^+$ level as a function of proton number.

V. CONCLUSIONS

A significantly improved low-spin level scheme for ^{137}Cs has been established from an experiment with a ^{136}Xe beam and a ^{10}B target, where particle-γ coincidence measurements with the PhoswichWall and the Digital Gammasphere detector arrays were carried out. As a result, knowledge on the sets of positive-parity levels associated with the single-particle proton states of the $50-82$ shell and with the members of the $\upsilon = 3$ $g_{7/2}$ multiplet has been considerably increased. In addition, new states have been observed including a candidate $13/2^+$ level. Two long-standing issues have been identified. First, among the positive-parity states, a predicted low-lying ($E \lesssim 1200$ keV) $3/2^+$ state is still missing. Second, the $E = 1868$-keV level has been reassigned as $I^\pi = 11/2^-$ (i.e., $h_{11/2}$) and this concurs with the $\ell = 5$ characterization of the state in earlier transfer-reaction work. Shell-model calculations performed in the course of this study reproduce the features of the detailed level scheme satisfactorily. A comparison of the ^{137}Cs levels with those of the lighter odd-proton, neutron-magic nuclei was presented, resulting in suggestions for follow-up γ-ray spectroscopic studies of these isotones.

Acknowledgments

The authors thank J. T. Anderson and M. B. Oberling (ANL) for technical support and J. P. Greene (ANL) for the preparation of the target. This work was supported by the U.S. Department of Energy, Office of Science, Office of Nuclear Physics under Grants number DE-SC0014442 (WU), DE-FG02-97ER41041 (UNC), and DE-FG02-97ER41033 (TUNL) and Contract numbers DE-AC02-06CH11357 (ANL) and DE-AC05-00OR22725 (ORNL). This research used resources of ANL's ATLAS facility, which is a DOE Office of Science User

Facility. E. P.-R. acknowledges financial support of PAPIIT IN110418.

[1] D. F. Geesaman, C. K. Gelbke, R. V. F. Janssens, and B. M. Sherrill, Annu. Rev. Nucl. Part. Sci. **56**, 53 (2006); and references therein.

[2] R. Broda *et al.*, Phys. Rev. C **59**, 3071 (1999).

[3] A. Astier *et al.*, Phys. Rev. C **85**, 064316 (2012).

[4] K. Li *et al.*, Phys. Rev. C **75**, 044314 (2007).

[5] B. H. Wildenthal, E. Newman, and R. L. Auble, Phys. Rev. C **3**, 1199 (1971).

[6] E. Monnand *et al.*, J. Phys. Rad. **36**, 1 (1975).

[7] W. R. Western *et al.*, Phys. Rev. C **15**, 1024 (1977).

[8] E. Browne and J. K. Tuli, Nucl. Data Sheets **108**, 2173 (2007).

[9] J. M. Allmond *et al.*, Phys. Rev. C **86**, 031307(R) (2012).

[10] W. Reviol *et al.*, Phys. Rev. C **94**, 034309 (2016).

[11] J. T. Anderson *et al.*, 2012 IEEE Nuclear Science Symposium and Medical Imaging Conference Record (NSS/MIC), N20-2, p. 1536; and references therein.

[12] The furthest downstream ring of Digital Gammasphere was not used.

[13] D. G. Sarantites, W. Reviol, J. M. Elson, J. E. Kinnison, C. J. Izzo, J. Manfredi, J. Liu, H. S. Jung, and J. Goerres, Nucl. Inst. Meth. A **790**, 42 (2015).

[14] K. J. Honkanen, F. A. Dilmanian, D. G. Sarantites, and S. P. Sorensen, Nucl. Inst. Meth. A **257**, 233 (1987).

[15] D. C. Radford, Nucl. Inst. Meth. A **361**, 297 (1995).

[16] An inspection of T. Yamazaki, Nucl. Data Tables A **3**, 1 (1967) indicates that the $B4F4$ values (representing the A_4 parameter) are zero for $3/2 \rightarrow 5/2$ ($L1 = L2 = 1$) and $3/2 \rightarrow 7/2$ ($L1 = L2 = 2$) transitions ($L1$ and $L2$ representing the angular momenta of the corresponding transition), but non-zero for the $7/2 \rightarrow 5/2$ ($L1 = L2 = 1$) and $7/2 \rightarrow 7/2$ ($L1 = L2 = 2$) cases. The use of the spin-alignment method in the present study implies that the angular-distribution coefficients have opposite signs compared to those in Yamazaki's tables.

[17] L. Coraggio, A. Covello, A. Gargano, and N. Itaco, Phys. Rev. C **87**, 021301(R) (2013).

[18] R. Machleidt, Phys. Rev. C **63**, 024001 (2001).

[19] H. Prade, W. Enghardt, H. Jäger, I. Käubler, H.-J. Keller, and F. Stary, Nucl. Phys. A **47**,

76 (1981).

[20] NNDC database, http://www.nndc.bnl.gov/nudat2.

[21] D. J. Rowe and J. L. Wood, Fundamentals of Nuclear Models, World Scientific (2010); see specifically Chapter 6.3.

TABLE I: Details of the experiments with a 560-MeV ^{136}Xe beam impinging on ^{13}C, ^{9}Be, and ^{10}B targets.

	^{13}C target	^{9}Be target	^{10}B target
Target thickness (mg/cm^2)	0.15	1.5	0.1
Mid-target energy (MeV)	553.9	503.0	556.2
Target purity (%)	99	100 [a]	>92
Duration (h)	40	14	21
Beam intensity (ppA)	500	70	500
Channel of interest	^{137}Xe + ^{12}C	^{137}Xe + ^{8}Be (2α)	^{137}Cs + ^{9}Be
Reference	[10]	[10]	This paper

[a]mono-isotopic.

TABLE II: Information on the energy levels and γ-ray transitions in ^{137}Cs from the present work.

E (keV) [a]	$I_i^\pi \rightarrow I_f^\pi$ [b]	E_γ (keV)	I_γ [c]	A_2/A_0	A_4/A_0
455.2(3)	$5/2^+ \rightarrow 7/2^+$	455.2(3)	100.0(30)	0.17(2)	−0.02(2)
848.6(4)	$5/2^+ \rightarrow 5/2^+$	393.4(3)	6.1(3)	−0.26(10)	0.07(15)
848.6(4)	$5/2^+ \rightarrow 7/2^+$	849.0(10)	21.0(36)	0.22(5)	−0.10(5)
1184.1(6)	$11/2^+ \rightarrow 7/2^+$	1184.1(6)	29.1(9)	−0.13(2)	0.04(2)
1273(1)	$9/2^+ \rightarrow 7/2^+$	1273.0(10) [d]	16.7(7)	0.21(5)	−0.07(4)
1492(2)	$1/2^+ \rightarrow 5/2^+$	1037.0(10) [e]	4.9(5)	0.00(13) [f]	
1564(2)	- $\rightarrow 5/2^+$	715.6(5) [g]	1.9(4)		
1564(2)	- $\rightarrow 5/2^+$	1109.0(20)	6.5(18)		
1570(2)	$9/2^+ \rightarrow 5/2^+$	1114.0(10) [d]	12.6(6)	−0.31(8)	0.02(8)
1570(2)	$9/2^+ \rightarrow 7/2^+$	1570.0(20)	12.1(7)	0.35(9)	−0.10(7)
1652(1)	$(5/2, 9/2) \rightarrow 5/2^+$	802.5(5) [g]	0.9(2)		
1652(1)	$(5/2, 9/2) \rightarrow 5/2^+$	1197.0(10) [d]	4.4(3)	−0.18(14) [f]	
1671(1)	$15/2^+ \rightarrow 11/2^+$	486.5(4)	13.2(9)	−0.32(11)	0.10(10)
1811(1) [h]	$13/2 \rightarrow 11/2^+$	627.1 (5) [e]	8.1(12)	0.33(15)	−0.06(12)
1868(2)	$11/2^- \rightarrow 9/2^+$	298.4(2) [d]	9.5(4)	0.20(5)	−0.01(4)
1868(2)	$11/2^- \rightarrow 9/2^+$	594.3(4)	5.3(4)	0.23(9)	−0.05(8)
1868(2)	$11/2^- \rightarrow 11/2^+$	683.7(5)	1.5(3)		
1893(1)	$17/2^+ \rightarrow 15/2^+$	222.2(3)	6.7(6)	0.22(3)	−0.05(3)
1917(1)	- $\rightarrow 5/2^+$	1068.0(10) [g]	2.3(5)		
2044(1)	$(15/2^+) \rightarrow 15/2^+$ [i]	372.5(4)	2.6(5)		
2044(1)	$(15/2^+) \rightarrow 11/2^+$ [i]	860.9(7)	4.6(8)		

TABLE II: (Continued.)

E (keV) [a]	$I_i^\pi \rightarrow I_f^\pi$ [b]	E_γ (keV)	I_γ [c]	A_2/A_0	A_4/A_0
2067(2)	$3/2^+ \rightarrow 5/2^+$	1612.0(20) [d]	18.5(6)	0.12(3)	−0.03(3)
2158(2)	$1/2^+ \rightarrow 1/2^+$	666.0(5) [e]	1.6(2)		
2158(2)	$1/2^+ \rightarrow 5/2^+$	1703.0(30) [e]	9.9(9)	0.17(19) [f]	
2360(3) [h]	- $\rightarrow 5/2^+$	1905.0(30) [e]	2.8(6)		

[a]Energy of the depopulated state.

[b]Spins and parities of states involved with the transition given in the third column.

[c]Relative γ-ray intensity of the transition normalized to 100 for the 455-keV transition.

[d]Newly assigned initial spin.

[e]Newly observed γ ray.

[f]No A_4 coefficient extracted.

[g]Seen in coincidence with the 393- and 849-keV transitions.

[h]Newly observed level.

[i]Assignment adopted from Ref. [3].

TABLE III: A comparison of calculated and experimental level energies in ^{137}Cs. The calculations have been performed assuming a ^{132}Sn core. The reduced transition probabilities reported in footnotes a and b have been obtained using g factors $g_l = 1.2$ and $g_s = 0.7\ g_{s,free}$. The configuration listed in the third column represents a coupling between the 0^+_1, 0^+_2, 2^+_1, 4^+_1, or 6^+_1 states of ^{136}Xe and a valence proton (see text).

calculations			*experiment*	
I^π	E (keV)	dominant configuration	I^π	E (keV)
$5/2^+_1$	444	$0^+_1 \otimes 1d_{5/2}$	$5/2^+$	455
$5/2^+_2$	1017	$2^+_1 \otimes 0g_{7/2}$	$5/2^+$	849
$3/2^+_1$	1202	$2^+_1 \otimes 0g_{7/2}$		
$11/2^+_1$	1353	$2^+_1 \otimes 0g_{7/2}$	$11/2^+$	1184
$9/2^+_1$	1390	$2^+_1 \otimes 0g_{7/2}$	$9/2^+$	1273
$15/2^+_1$	1679	$4^+_1 \otimes 0g_{7/2}$	$15/2^+$	1671
$7/2^+_2$	1742	$2^+_1 \otimes 1d_{5/2}$		
$9/2^+_2$ [a]	1745	$2^+_1 \otimes 1d_{5/2}$	$9/2^+$	1570
$1/2^+_1$	1750	$2^+_1 \otimes 1d_{5/2}$	$1/2^+$	1492
$3/2^+_2$ [b]	1774	$0^+_1 \otimes 1d_{3/2}$, $2^+_1 \otimes 1d_{5/2}$ [c]	$3/2^+$	2067
$11/2^-$	1776	$0^+_1 \otimes 0h_{11/2}$	$11/2^-$	1868
$5/2^+_3$	1799	$2^+_1 \otimes 1d_{5/2}$	$(5/2, 9/2)$	1652
$7/2^+_3$	1887	$0^+_2 \otimes 0g_{7/2}$		
$3/2^+_3$	1925	$0^+_1 \otimes 1d_{3/2}$, $2^+_1 \otimes 1d_{5/2}$ [c]		
$13/2^+$	1953	$4^+_1 \otimes 1d_{5/2}$	13/2	1811
$11/2^+_2$	1985	$4^+_1 \otimes 1d_{5/2}$		
$17/2^+$	2021	$6^+_1 \otimes 1d_{5/2}$	$17/2^+$	1893
$1/2^+_2$	2159	$0^+_1 \otimes 2s_{1/2}$	$1/2^+$	2158
$15/2^+_2$	2178	$6^+_1 \otimes 1d_{5/2}$	$(15/2^+)$	2044

[a] Strong $9/2^+_2 \rightarrow 7/2^+_2$ transition predicted [$B(M1) = 0.3\ \mu_N^2$].
[b] Strong $3/2^+_2 \rightarrow 5/2^+_1$ transition predicted [$B(M1) = 0.9\ \mu_N^2$].
[c] Mixed configuration (the two components contribute about equally to the total wavefunction).

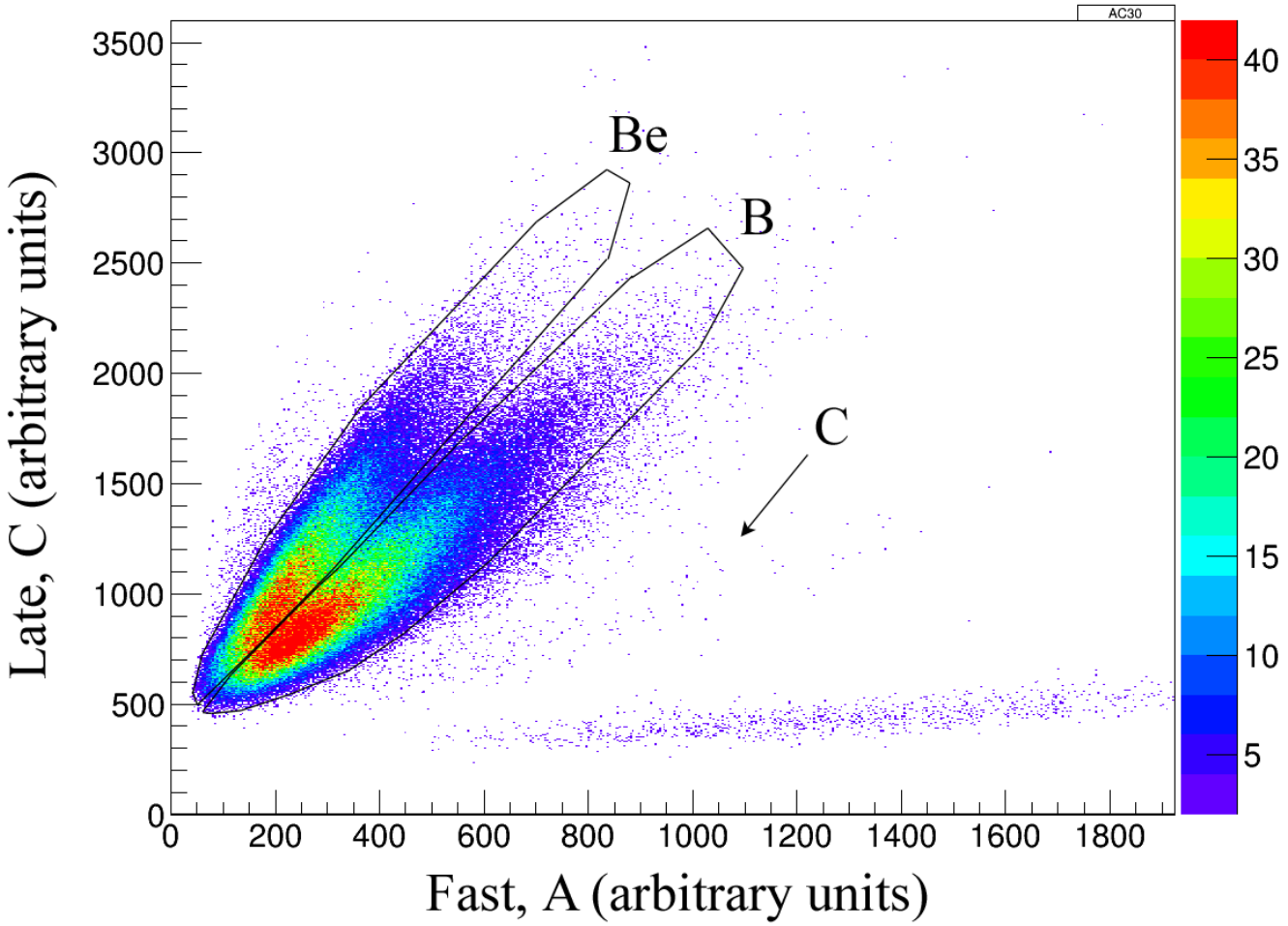

FIG. 1: An (A,C) particle map for the ^{136}Xe + ^{10}B data. The study of ^{137}Cs uses the two-dimensional gate that selects beryllium events. The two other particle groups represent boron and carbon events, respectively, the former being associated with projectile Coulomb excitation. The map is for pixel 30 of the Phoswich Wall. The color scale shown on the right provides the range of z-axis values in this example.

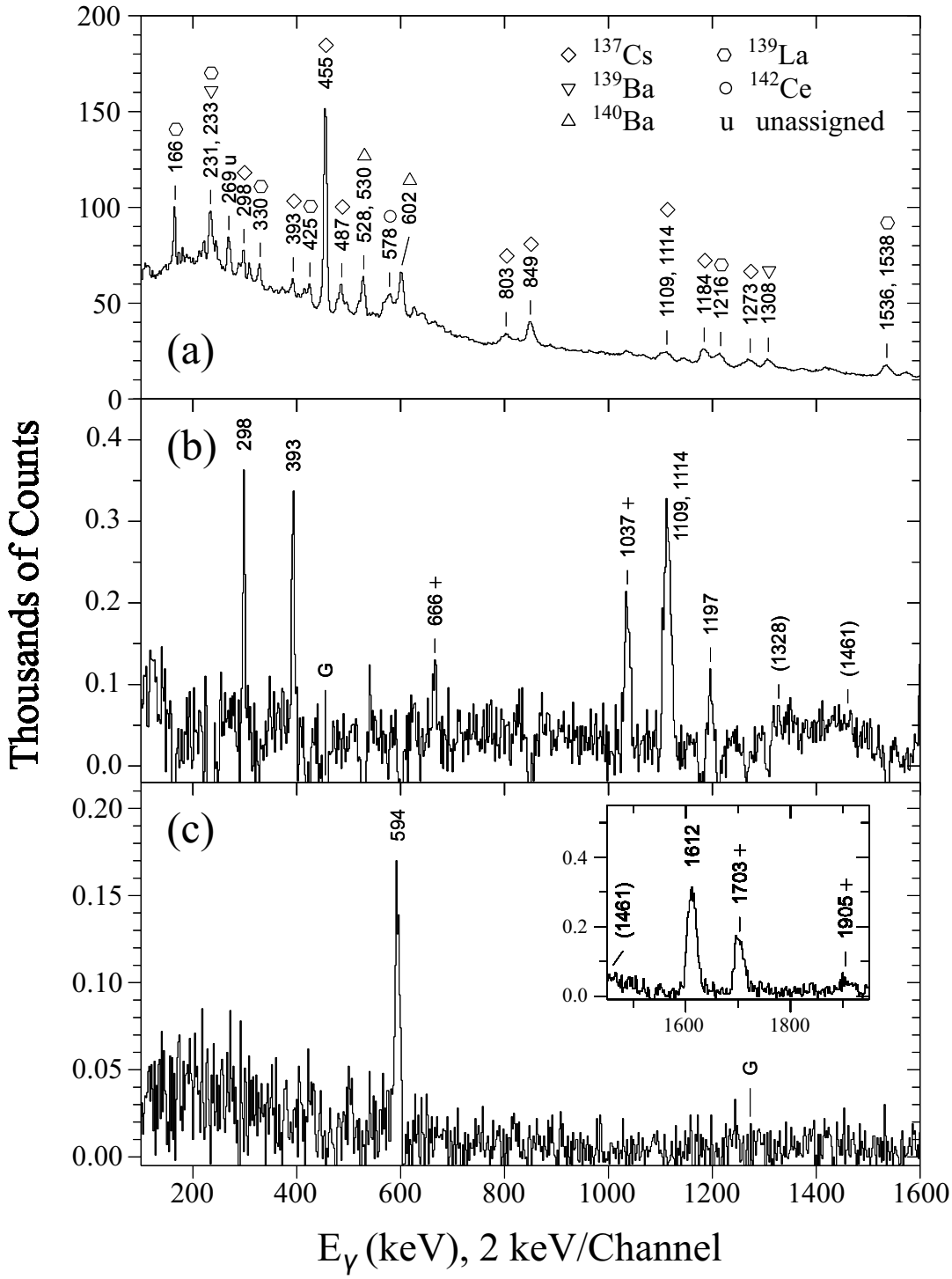

FIG. 2: Representative γ-ray spectra for the 560-MeV ^{136}Xe + ^{10}B reaction. (a) Total projection of a γ-γ coincidence matrix gated by beryllium ions in the A-C map (see text). Transitions are labeled by their energy in keV. (b) Coincidence spectrum for ^{137}Cs obtained by gating on the 455-keV transition. Transitions with labels in parentheses are viewed as insignificant (see text). (c) Similar to (b), but for the 1273-keV gating transition (main panel). Inset: higher-energy extension of the spectrum of panel (b). The position of the gate is always indicated by the letter G. The γ rays labeled by a plus sign are newly observed.

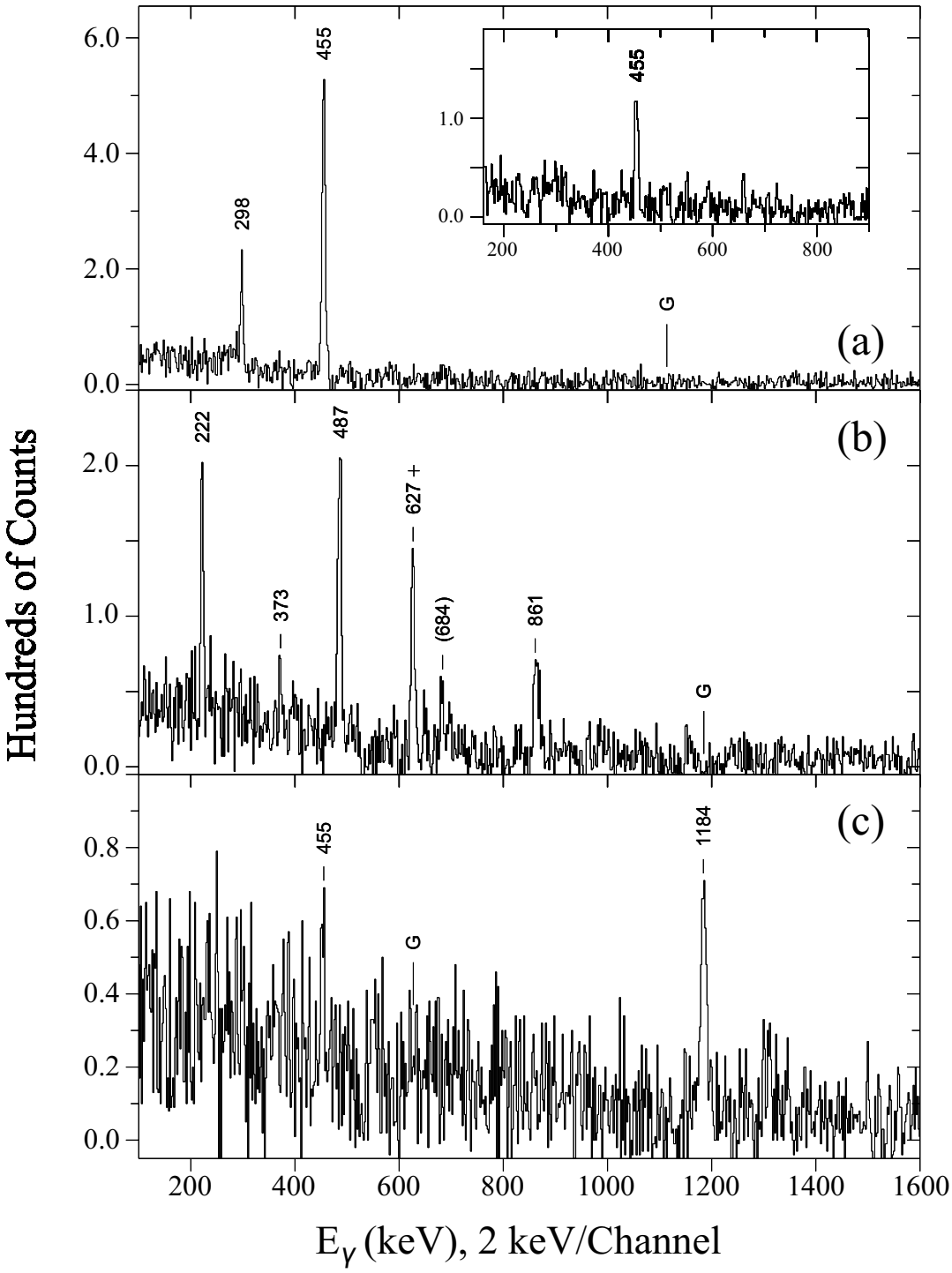

FIG. 3: Coincidence spectra for ^{137}Cs obtained by gating on the transitions with the respective energies of (a) 1114 keV (main panel) and 1109 keV (inset) , (b) 1184 keV, and (c) 627 keV. The meaning of G and of the plus sign is the same as in Fig. 2. The 684-keV assignment in panel (b) is done with less confidence than that for a stronger peak.

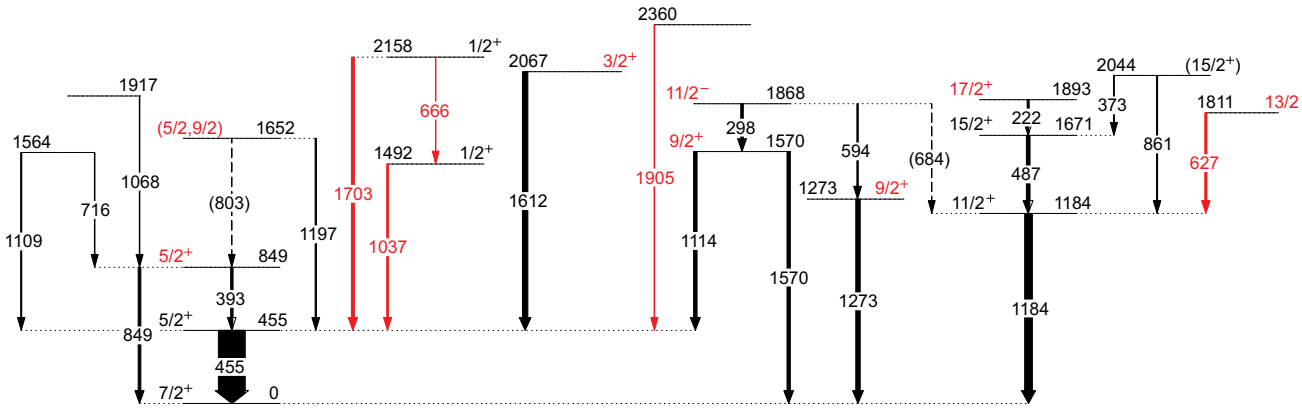

FIG. 4: (Color online) The level scheme for ^{137}Cs obtained in the 560-MeV ^{136}Xe + ^{10}B reaction. The widths of the arrows are proportional to the measured γ-ray intensities. The energies are given in keV. The assignments given in parentheses are tentative. The transitions and the spin-parity assignments marked in red are new to this work.

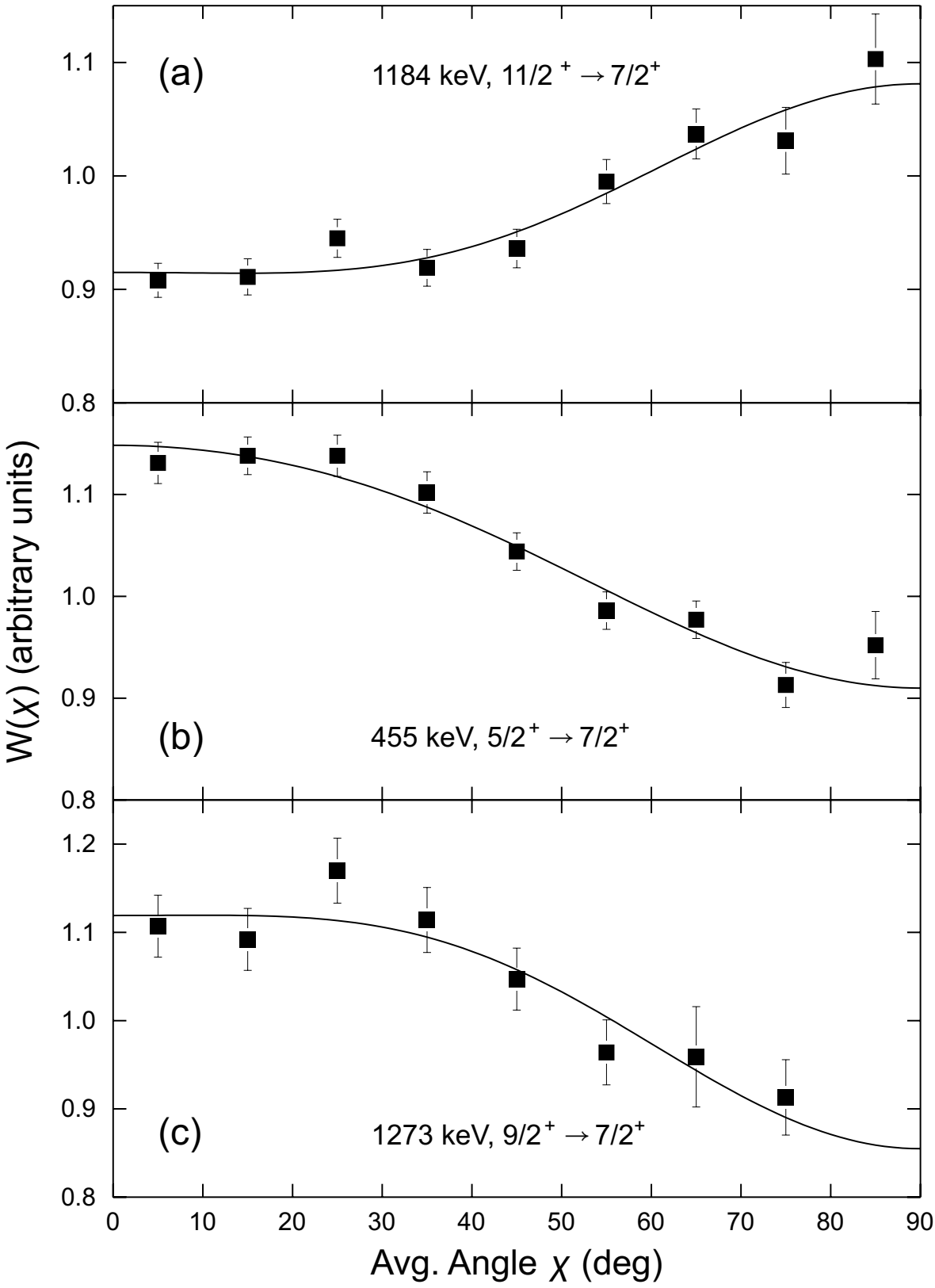

FIG. 5: Representative γ-ray angular distributions, with respect to the spin direction, for transitions in ^{137}Cs. Panels (a) - (c) are for the 1184-, 455-, and 1273-keV transitions, respectively. The former two cases are established stretched-quadrupole ($E2$) and antistretched magnetic-dipole ($M1$) transitions, respectively.

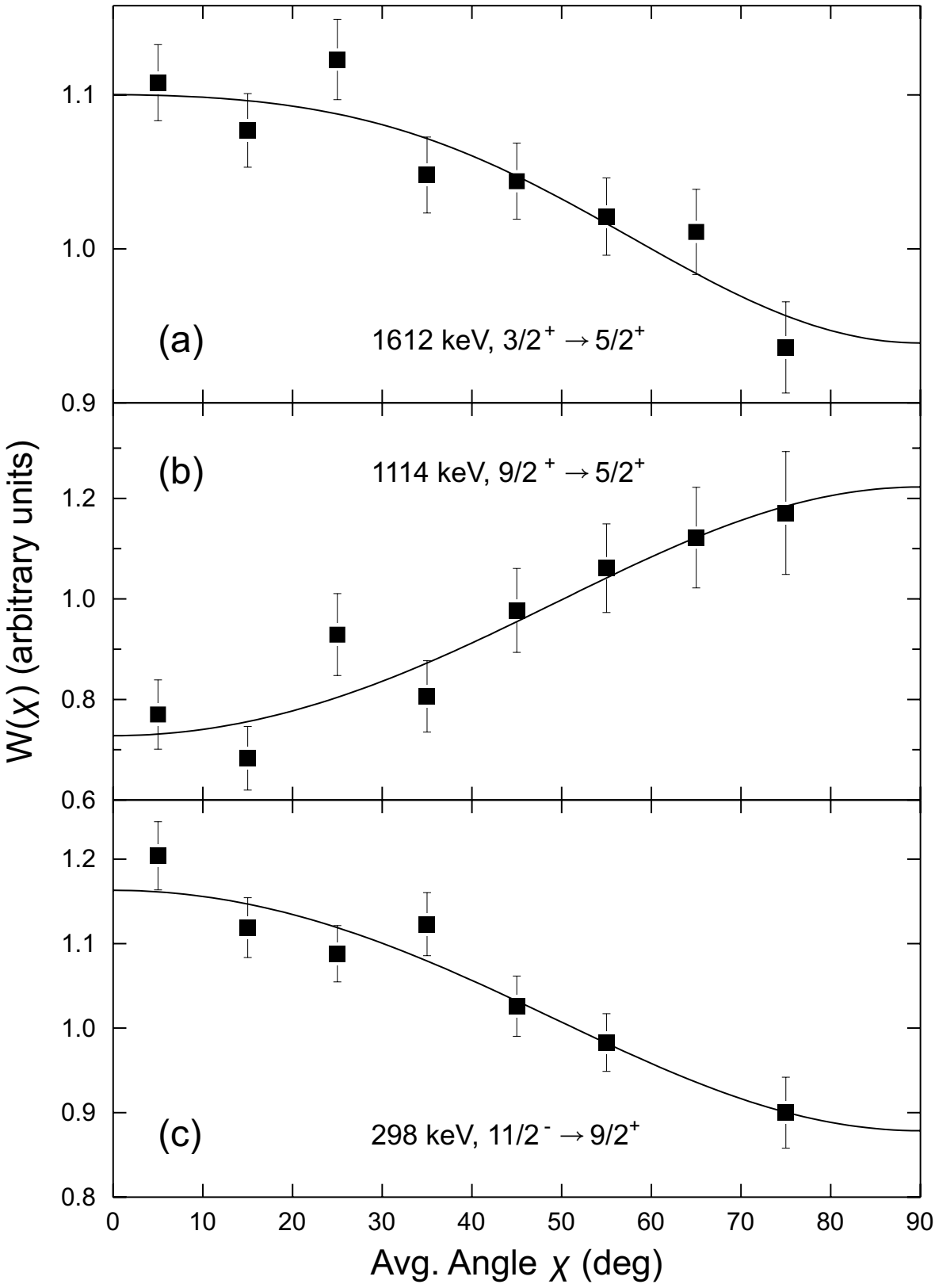

FIG. 6: Similar to Fig. 5, but for the (a) 1612-, (b) 1114-, and (c) 298-keV transitions. For all these transitions, new spin-parity assignments are proposed.

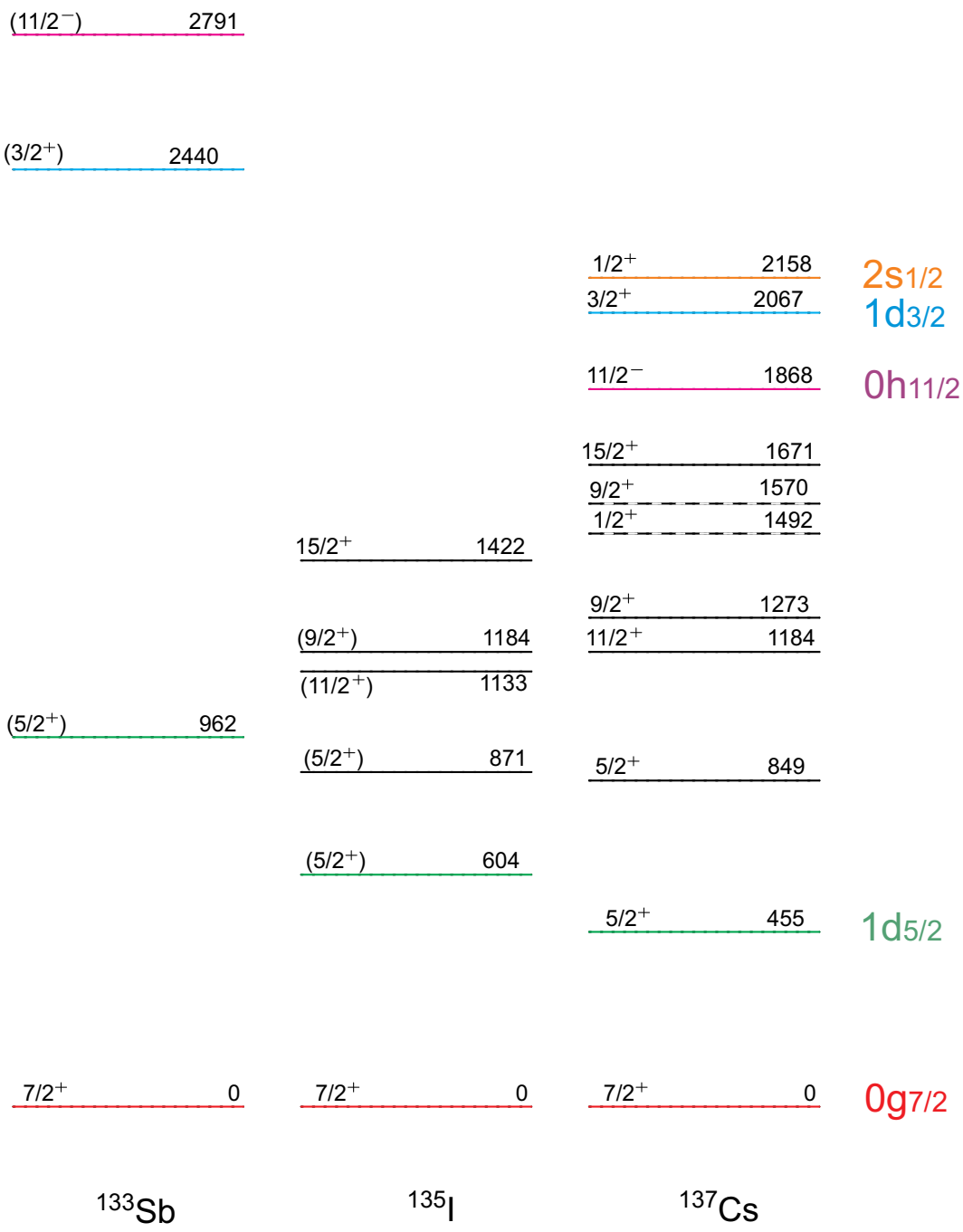

FIG. 7: The lowest-spin levels in the $N = 82$ ^{133}Sb,^{135}I, and ^{137}Cs nuclei. The information on the former two isotones is adopted from Ref. [20]. States with spins above 11/2 in ^{133}Sb and 15/2 in ^{135}I and ^{137}Cs have been omitted. The spins and parities given in parentheses represent tentative assignments. The sets of levels in black are part of the seniority $\upsilon = 3$ $0g_{7/2}$ (full line) and $\upsilon = 3$ $0g_{7/2}1d_{5/2}$ multiplets (dashed line). The levels in color are single-proton ($\upsilon = 1$) states, and their configurations are given on the right-hand side. See text for details.